Vegetation effects on the isotope composition of oxygen in atmospheric CO_2

Graham D. Farquhar*, Jon Lloyd*, John A. Taylor†, Lawrence B. Flanagan‡, James P. Syvertsen§, Kerry T. Hubick*, S. Chin Wong* & James R. Ehleringer||

* Plant Environmental Biology Group, Research School of Biological Sciences, Institute of Advanced Studies, Australian National University, GPO Box 475, Canberra, ACT 2601, Australia
† Centre for Resource and Environmental Studies, Institute of Advanced Studies, Australian National University, Canberra, ACT 2601, Australia
‡ Department of Biology, Carleton University, 1125 Colonel By Drive, Ottawa K1S 5B6, Ontario, Canada
§ Citrus Research and Education Center, University of Florida, Lake Alfred, Florida 33850, USA
|| Department of Biology, University of Utah, Salt Lake City, Utah 84112, USA

THE $^{18}O/^{16}O$ ratio in atmospheric CO_2 is a signal dominated by CO_2 exchange with the terrestrial biosphere and it has considerable potential to resolve the current importance of the oceans and individual terrestrial biomes as net sinks for anthropogenic CO_2. Fractionation of the oxygen isotopes of CO_2 occurs in plants owing to differential diffusion of $C^{18}O^{16}O$ and $C^{16}O_2$ and to isotope effects in oxygen exchange with chloroplast water. Here we investigate the consequences of these effects for the global distribution of oxygen isotopes in CO_2. We predict that ^{18}O isotopic exchange fluxes, especially between the atmosphere and terrestrial biosphere, are large, with considerable spatial variation. Near 70° N, where precipitation (and soil water) is most depleted in ^{18}O, photosynthesis and respiration both deplete the atmospheric CO_2 of ^{18}O. This provides an explanation for the depletion of ^{18}O in atmospheric CO_2 at high northern latitudes[1].

During terrestrial photosynthesis, heavier $C^{18}O^{16}O$ molecules diffuse into leaves more slowly than do the lighter $C^{16}O_2$. Further, within the chloroplasts, carbonic anhydrase catalyses the exchange of oxygen atoms between CO_2 and the water there. The $^{18}O/^{16}O$ ratio of chloroplast water is enriched compared with soil water because $H_2{}^{18}O$ evaporates more slowly from leaves than does $H_2{}^{16}O$. Some of the CO_2 entering the chloroplast and exchanging oxygen atoms with chloroplast water is assimilated via photosynthesis, but some diffuses back into the atmosphere, the amount depending on the concentration of CO_2 in the chloroplast and on conductances to diffusion within and from the leaf. CO_2 molecules diffusing out of the leaf after exchanging oxygens are usually, but not always, enriched in ^{18}O compared to those in the ambient air. CO_2 released in respiration and decomposition is less enriched because it largely reflects CO_2 in equilibrium with unenriched soil water.

The ^{18}O composition of water at the sites of evaporation within leaves, δ_E, is enriched with respect to source (soil) water. Following the derivation for a free water surface[2], an equation for δ_E can be presented[3]

$$\delta_E = \delta_S + \varepsilon_k + \varepsilon^* + (\delta_v - \delta_S - \varepsilon_k)\frac{e_a}{e_i} \quad (1)$$

where δ_S is the isotope composition of source water, δ_V is the isotopic composition of water vapour in the surrounding air, e_a and e_i are the vapour pressures in the atmosphere and intercellular spaces, ε^* is the proportional depression of equilibrium vapour pressure by the heavier molecule (9.2‰ at 25 °C; ref. 4) and ε_k is the kinetic fractionation factor, 28.5‰ for diffusion through stomata[5] and 18.9‰ in the boundary layer[3]. Liquid $H_2{}^{18}O$ is concentrated at the evaporating sites and so diffuses away from them in the liquid phase, relative to $H_2{}^{16}O$. This is opposed by convection of source water into the leaf, a Péclet effect. Therefore bulk leaf water, δ_L, is less enriched in ^{18}O than water at the evaporating sites. Most solar energy absorption occurs in chloroplasts and evaporation is from the adjacent air–water interfaces[6]. The ^{18}O composition of water in the chloroplasts should therefore be closer to δ_E than to δ_L.

The enrichment in ^{18}O in chloroplast water will be passed to CO_2, with interconversion being catalysed by the enzyme carbonic anhydrase with an equilibrium fractionation factor of 41.2‰ at 25 °C (ref. 7). The CO_2 can then be assimilated (at net rate A) or diffuse out of the leaf. The resulting isotope composition of CO_2 in the chloroplast, δ_C, affects the isotope discrimination against ^{18}O during net CO_2 assimilation. We define this discrimination, Δ_A, as $R_a/R_A - 1$, where R_a is the $^{18}O/^{16}O$ ratio of ambient CO_2, and R_A is that ratio for the net flux of CO_2 into the leaf. This definition, based on the net rate of assimilation, A (that is, consumption of CO_2), is general enough to include possible effects of the carboxylating enzyme, but in what follows

Symbols used in text

$\bar{a}$	Weighted mean of discriminations occurring during the diffusion of CO_2 from ambient air to the sites of carboxylation
a_w	Fractionation against $C^{18}O^{16}O$ (compared to $C^{16}O_2$) during dissolution and diffusion in water
A	Net rate of CO_2 assimilation (=GPP at regional or global level)
c_a	Mole fraction of CO_2 in air
C_a	Atmospheric partial pressure of CO_2 (pCO_2)
C_c	pCO_2 in chloroplast
C_{st}	pCO_2 in substomatal cavities
D	Leaf-to-air vapour pressure difference
δ_a	Oxygen (O) isotope composition of atmospheric CO_2 relative to PDB-CO_2
δ_{an}	O isotope composition of CO_2 released anthropogenically (PDB-CO_2 scale)
δ_c	O isotope composition of CO_2 in chloroplast (PDB-CO_2 scale)
δ_E	O isotope composition of water at sites of evaporation in leaf (SMOW scale)
δ_L	O isotope composition of bulk leaf water (SMOW scale)
δ_o	O isotope composition of water in the ocean (SMOW scale)
δ_p	O isotope composition of precipitation (SMOW scale)
δ_r	O isotope composition of respired CO_2 (PDB-CO_2 scale)
δ_s	O isotope composition of water in soil (SMOW scale)
δ_v	O isotope composition of water vapour in air (SMOW scale)
Δ_A	Discrimination against ^{18}O (compared to ^{16}O) during net CO_2 assimilation
e_a	Ambient water vapour pressure
e_i	Water vapour pressure in intercellular spaces of leaves
E_v	Elevation
ε_k	Kinetic fractionation against $H_2{}^{18}O$ compared to $H_2{}^{16}O$ during diffusion in air
ε^*	Proportional depression of vapour pressure of $H_2{}^{18}O$ compared to $H_2{}^{16}O$
F_{an}	Molar flux of CO_2 to atmosphere from anthropogenic sources
F_{ao}	Gross (one way) molar flux of CO_2 from atmosphere to ocean
F_{oa}	Gross molar flux of CO_2 from ocean to atmosphere
ϕ_c	Proportion of A lost in plant respiration
g	Conductance to diffusion of CO_2 from atmosphere to chloroplasts
GPP	Gross primary productivity (molar carbon flux)
Γ	CO_2 compensation point
λ	Lagrange multiplier representing the marginal water cost of plant carbon gain
M	Number of moles of air in the atmosphere
NPP	Net primary productivity (molar carbon flux)
P_a	Annual precipitation
PDB-CO_2	CO_2 formed by addition of phosphoric acid to Pee Dee Belemnite calcite
$\mathfrak{R}$	Molar flux of CO_2 released by plant and soil respiration
R_a	$^{18}O/^{16}O$ ratio of CO_2 in ambient air
R_A	$^{18}O/^{16}O$ ratio of the net flux of CO_2 into the leaf
SMOW	Standard mean ocean water
T	Annual mean temperature
T_1	Leaf temperature
T_m	Monthly mean air temperature

we show that such effects are small and that the discrimination is effectively dominated by fractionation during diffusion and by the CO_2-water exchange reaction.

Following analogous derivations[8] for $^{13}CO_2$, we obtain an equation for ^{18}O discrimination in the case of complete isotopic equilibration between CO_2 and water before the fixation of CO_2

$$\Delta_A = \bar{a} + \frac{C_c}{C_a - C_c}(\delta_c - \delta_a) \quad (2)$$

where δ_a is the isotope composition of the ambient CO_2, C_c and C_a are the partial pressures of CO_2(pCO_2) in the chloroplast and ambient air, respectively, and $\bar{a}$ is the weighted mean of discriminations occurring during the diffusion from ambient air to the sites of carboxylation within the chloroplast. The value of $\bar{a}$ will be dominated by fractionation during diffusion from the leaf surface to the mesophyll cell wall (8.8‰, based on the reduced mass of CO_2 and air) but also includes smaller fractionations in the laminar boundary layer and during diffusion through solution. We estimate $\bar{a}$ to be ~7.4‰.

Figure 1 shows the relationship between Δ_A and C_c/C_a for leaves of C_3 tree species, for which on-line ^{13}C discrimination has been measured and analysed[9]. Also shown are the relationships between Δ_A and C_c/C_a for chloroplast water having the same composition as source water ($\delta_S = -8.0$‰ SMOW) and for water at the evaporating surface within the leaf. In both cases, equilibrium between CO_2 and H_2O is assumed. Values of Δ_A observed are close to CO_2 in full equilibrium with water at the sites of evaporation. Data shown in Fig. 1 are from woody species but similar results were obtained for wheat and soybean in Canberra and *Phaseolus vulgaris* in Utah. CO_2 produced from respiration and photorespiration can be less enriched than is expected for CO_2 in full equilibrium with δ_E (ref. 10). Nevertheless, isotope exchange during CO_2 assimilation is well predicted using equation (2). $A\Delta_A$ can then simply be regarded as the net result of a flux, gC_a, into the leaf with an isotopic source δ_a (g being the conductance to diffusion), and a flux, gC_c, out of the leaf with the isotope source, δ_c, being equivalent to that for full equilibrium between CO_2 and evaporating surface water. Each flux is subject to discrimination, $\bar{a}$, during diffusion.

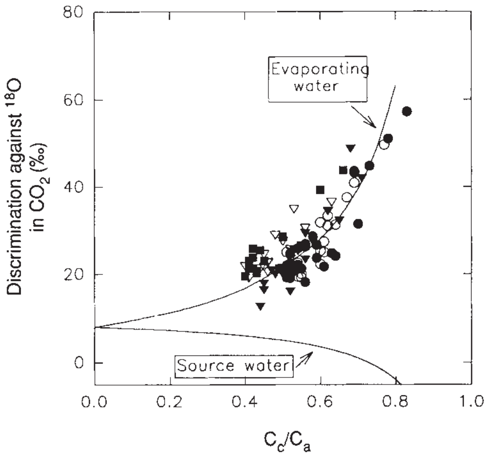

FIG. 1 Relationship between discrimination against $C^{18}O^{16}O$ (Δ_A) and the ratio of chloroplastic to ambient partial pressures of CO_2 (C_c/C_a) for C_3 tree species grown under conditions of either full sunlight or under shade cloth. Full experimental details related to ^{13}C discrimination have been provided[9]. The estimates of C_c used here are those obtained from ^{13}C discrimination, but with the internal conductance for CO_2 diffusion within the leaf multiplied by 0.7 to account for C_c estimates from $^{13}CO_2$ discrimination being weighted by assimilation rates, and C_c values appropriate for $C^{18}O^{16}O$ discrimination being weighted by diffusion conductances (see appendices 1 and 2 of ref. 9). ■, Sun peach (*Prunus persica*); ▼, shade peach; □, sun grapefruit (*Citrus paradisi*); ∇, shade grapefruit; ○, sun lemon. Also shown are the values expected if CO_2 were in full equilibrium with source water ($\delta^{18}O_{SMOW} = -8.0$‰) or in full equilibrium with water at the evaporating surface ($\delta^{18}O_{SMOW} = +7$‰ at 25 °C and $D = 1.1$ kPa). $\delta^{18}O_{PDB}$ of CO_2 entering the leaf chamber was typically −7‰. (Canberra).

To calculate Δ_A on a global basis, we first estimated soil water isotope composition which reflects the precipitation (δ_P) with seasonal variability in δ_P almost completely dampened[11,12]. It was calculated by regressing δ_P for sites in the IAEA network[13] against annual mean temperature, T (°C), annual precipitation, P_a(m) and elevation, E_v(m). The best fit obtained was

$$\delta_P\,(\text{SMOW}) = (0.579T - 0.0114T^2 - 1.35P_a + 4.47P_a^2 - 0.147\sqrt{E_v} - 9.80) \times 10^{-3}$$

With δ_P simulated at 2.5° resolution using temperature[14], precipitation[15] and elevation[16] fields, the result is shown in Fig. 2. To calculate δ_E, ε_k was taken as 26‰ and ($\delta_V - \delta_S$) was calculated from simulations of the global $H_2{}^{18}O$ atmospheric cycle[17] for continental regions, taking monthly values of δ_v and annual precipitation-weighted values of δ_s. Leaf temperature (T_l) was calculated as $T_l = 1.05(T_m + 2.5°)$. The 2.5° addition accounts for a daytime increase in air temperature over monthly mean air temperature (T_m) and the 5% allows for net canopy to air heat fluxes. Monthly relative humidities were calculated using dewpoint temperatures and adding 1 °C to account for higher daytime vapour pressures.

We then used δ_a for 1985[1], constant at +0.77‰ between 90° S and 32° S, then decreasing linearly with latitude to −1.37‰ at 90° N. δ_c was taken as the value for CO_2 in full equilibrium with δ_E, and Δ_A was then obtained from equation (2) with $\bar{a} = 7.4$‰, allowing C_c/C_a to vary with leaf-to-air vapour pressure difference, D. We first calculated C_{st}, the pCO_2 in the substomatal cavities, using a simple stomatal model[18] as $C_{st}/C_a = 1 - \sqrt{\{1.6D(C_a - \Gamma)/(\lambda C_a^2)\}}$, where Γ is the CO_2 compensation point and λ is a Lagrange multiplier[19] dependent upon vegetation type and photosynthetic mode as defined by a 1° resolution data set of land cover[20]. $(C_{st} - C_c)/C_a$ was taken as 0.1 (ref. 9). On a regional scale there are variations in temperature, δ_S (Fig. 2), relative humidity and C_c/C_a that cause Δ_A to vary (Fig. 3) from −20‰ in arctic tundra to +32‰ in the dry steppes of Kazakhstan and Ukraine. In the arid areas of Africa and Australia, Δ_A is low owing to the dominance of C_4 species with low C_c/C_a.

To assess the impact of discrimination against $C^{18}O^{16}O$ on a global scale, we then calculated a globally averaged Δ_A, weighted by CO_2 assimilation (gross primary productivity: GPP). Net primary productivity (NPP) was first related to temperature and precipitation[21,22] but with NPP = 0 in months where mean air temperature was less than −5 °C. A (=GPP) and NPP are related; $A = \text{NPP}/(1 - \phi_c)$, where ϕ_c is the proportion of A lost in plant respiration. We took into account the variation in ϕ_c, which ranges from 0.3 to 0.5 for herbaceous species[23,24], is 0.3–0.6 for temperate zone forests[25] and 0.65–0.80 for tropical forests[26]. ϕ_c has been estimated and GPP values converted to a carbon basis[27] using land cover data[20]. We estimate GPP to be 12.5 Pmol C yr^{-1} (where 1 Pmol C = 12×10^9 ton C), with 16% of the total by C_4 plants. Weighting according to GPP gives $\delta_S = -7.9$‰ (SMOW), $\delta_v = -18.2$‰ (SMOW), relative humidity at the leaf surface = 0.65, $\delta_E = +4.4$‰ (SMOW), $C_c/C_a = 0.57$, and $\Delta_A = 13.7$‰.

Uncertainty in C_c/C_a has the greatest potential impact on model results: a change of 1 p.p.m. in C_c will cause a change of almost 0.1‰ in the calculated Δ_A. The ratio C_c/C_a is, however, a reasonably conservative parameter, depending mostly on plant photosynthetic mode and D[6,18,19]. These effects are accounted for in the current model. Upon development of soil water deficits, C_c/C_a can decline[6,19]. Nevertheless, under such circumstances A is low and hence contributes little to the GPP-weighted value calculated here. Furthermore, in productive regions that regularly experience soil water deficits, the vegetation is often dominated by C_4 grasses. As can be seen from Fig. 1, Δ_A is less sensitive to C_c/C_a at lower values of that ratio, such as are typically found in C_4 plants. Plant $\delta^{13}C$ values can be used to estimate C_c of C_3 species[8,9]. Further data from around the globe will help constrain this uncertainty.

The other significant source of uncertainty is $(\delta_V - \delta_S)$, with a 1‰ error in our estimate causing a 1‰ change in Δ_A for globally averaged conditions. The GPP-weighted value we calculate here (−10.3‰) is close to that usually observed[28-31]. Uncertainties in the estimation of leaf temperatures introduce only minor inaccuracies into the calculations, and estimates of Δ_A are relatively insensitive to the calculated relative humidity. This is because the stomatal model interacts with D. The reduction in C_c/C_a accompanying a decrease in atmospheric humidity counters the increase in δ_E.

With GPP = 12.5 Pmol yr^{-1} and an atmospheric CO_2 pool of 62.5 Pmol, we estimate a global exchange time of 5 years for the carbon atom, and with $C_c/C_a = 0.57$, only 2.2 years for the oxygen atoms in CO_2. This is much faster than the exchange of oxygen atoms with the ocean (8.3 years). The ^{18}O content of atmospheric CO_2 is also influenced by release of CO_2 from soils and plants via respiration and release of CO_2 from fossil fuel and biomass burning[1,32]. Therefore, as already done for $^{13}CO_2$ (ref. 33), we can write

$$Mc_a \frac{d\delta_a}{dt} = F_{oa}(\delta_o - a_w - \delta_a) + F_{ao}a_w + \Re(\delta_r - \delta_a) + A\Delta_A + F_{an}(\delta_{an} - \delta_o) \qquad (3)$$

where M is the number of moles of air in the atmosphere, c_a

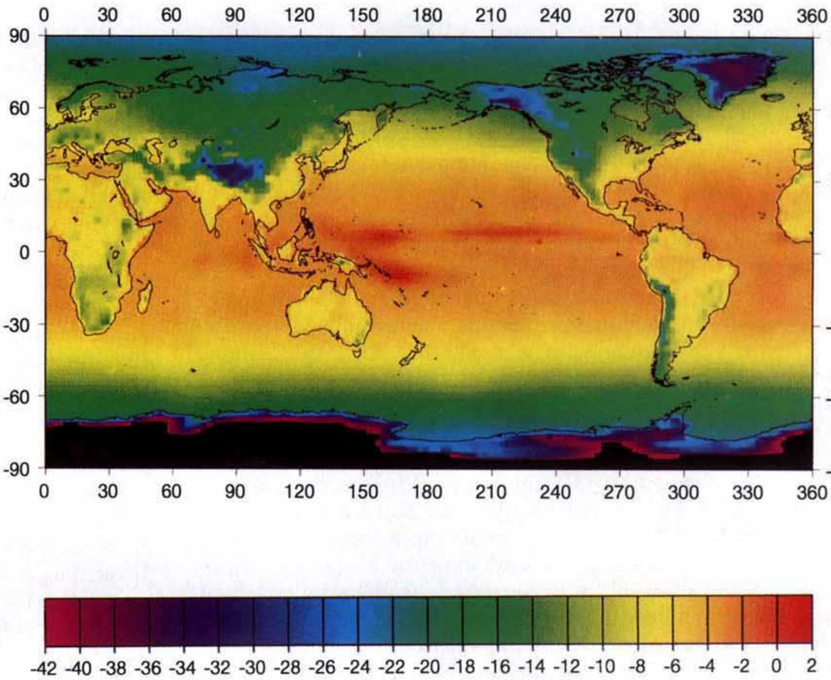

FIG. 2 Precipitation-weighted isotopic composition (SMOW) of precipitation.

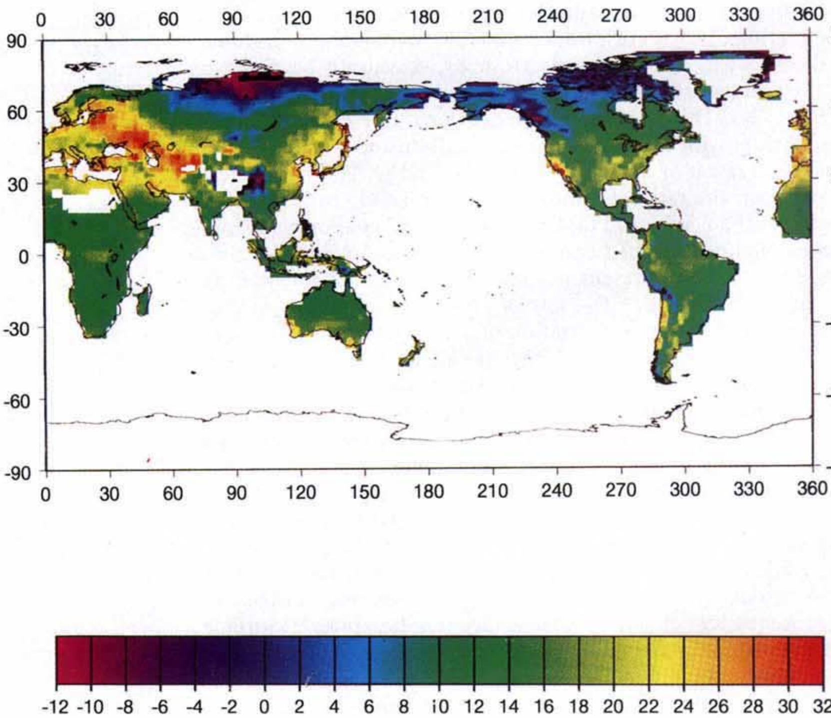

FIG. 3 Estimated mean annual values for discrimination against ^{18}O in CO_2 (Δ_A). Empty grid squares are modelled to have no terrestrial productivity.

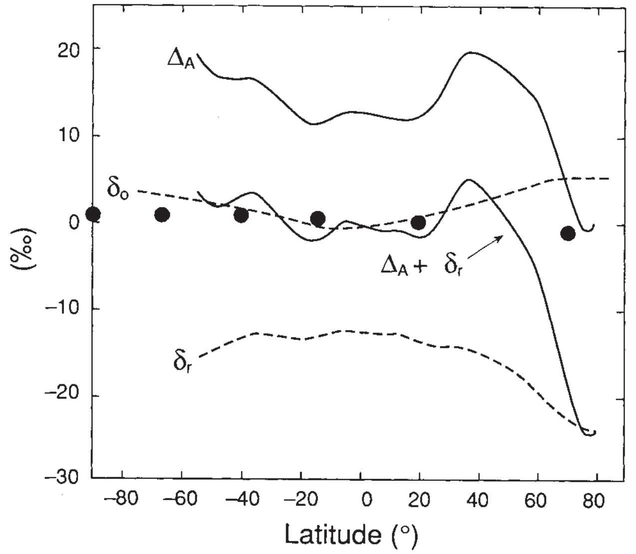

FIG. 4 10° latitudinal averages, weighted by GPP, of the predicted discrimination against ^{18}O in CO_2 (Δ_A), $\delta^{18}O$ (PDB-CO_2) of: respired CO_2 (δ_r), the sum $\Delta_A + \delta_r$, CO_2 in equilibrium with the ocean (δ_o) and mixed atmospheric CO_2 (δ_a data from ref. 1).

is the mole fraction of CO_2 in the atmosphere, F_{oa} and F_{ao} are the annual gross (one way) molar fluxes of CO_2 between oceans and atmosphere and atmosphere and oceans, $\Re$ is the annual gross flux for CO_2 released from plant and soil respiration, A is the flux of CO_2 associated with photosynthetic CO_2 assimilation (gross primary productivity, GPP) and F_{an} is the influx of CO_2 from anthropogenic sources. δ_o is the isotopic compositon of CO_2 in equilibrium with ocean water, δ_r is the isotopic composition of CO_2 respired by plants and soils as it enters the atmosphere, δ_{an} is the isotopic composition of anthropogenic CO_2, and a_w is the combined solubility/aqueous diffusion fractionation for $C^{18}O^{16}O$.

Solution of equation (3) requires $d\delta_a/dt$, and the effective sink terms, $(F_{ao} - F_{oa})$ and $(A - \Re)$. We solve a simpler case (effectively pre-anthropogenic), assuming a steady state with $F_{oa} = F_{ao}$, $A = \Re$, and $F_{an} = 0$, and solve for δ_r, taking[34] $F_{oa} = F_{ao} = 7.5$ Pmol yr^{-1}. δ_o was analysed from salinity[35] and sea-surface temperatures[35] using surface-water salinity/$\delta^{18}(H_2O)$ relationships[2], calculating the isotopic composition of CO_2 (PDB-CO_2 scale) in equilibrium with ocean water (SMOW scale)[36,37] at 2.5° resolution. This gives $\delta_o = +1.25$‰. Weighted according to cosine of latitude, $\delta_a = +0.18$‰. From inspection of equation (3), with respiration and GPP in balance on a global scale, because δ_a differs little from δ_o, δ_a should be close to $\Delta_A + \delta_r$. Indeed, from equation (3) we calculate that $\delta_r = -14.0$‰ (PDB-CO_2). This is 1.2‰ enriched compared with CO_2 in full equilibrium with soil water[12,38], −6.4‰, followed by 8.8‰ depletion[12] as a result of slower diffusion of $C^{18}O^{16}O$. This may reflect in part that the ratio of atmospheric to soil CO_2 concentration is greater than zero, and that soil water at the evaporating front can be slightly enriched compared to bulk soil water. We conclude that for the present purposes, δ_r is well represented by δ_p, equilibrated with CO_2, minus 7.6‰.

Using the last parameterization of δ_e, 10° latitudinal averages of Δ_A and δ_r (weighted by GPP) were calculated and are presented, with their sum, in Fig. 4, together with δ_o and δ_a. The significance of the sum lies in the future use of this model to predict local δ_a. This will require the linking of surface isotope exchange with an atmospheric mixing model. The local values of δ_a will be smoothed compared with the local isotope 'equilibrium values' (δ_{eq}) that would occur if there were no mixing. For oceans, $\delta_{eq} = \delta_o$, and for the terrestrial biosphere, $\delta_{eq} = (\Delta_A + \delta_r)$. Surface isotope effects will be dominated south of 20° S by oceans, and we note that δ_o increases with latitude as a consequence of lower sea-surface temperatures[2]. Surface effects will be increasingly dominated by the terrestrial biosphere up to 65° N. At this scale, Δ_A and δ_r tend to mirror each other over much of the globe (when averaged annually over a 10° band), but there is considerable disequilibrium at high northern latitudes. $(\Delta_A + \delta_r)$ decreases markedly above 45° N to a minimum in the 70°–80° N band (Fig. 4). This is largely a consequence of more negative δ_S (Fig. 2). It is consistent with, and provides an explanation for, measurements of mixed atmosphere δ_a (ref. 1), in which there was a meridional gradient (with strong depletion at 71° N) that required an enormous isotope exchange flux to maintain.

For any particular biome there is no unique relationship between Δ_A and δ_r, and the seasonal cycle in δ_a at most locations should not therefore have a unique relationship with pCO_2. This is in contrast to $^{13}CO_2$ and is consistent with variability in diurnal[39], seasonal[32,40] and annual[1] δ_a. Nevertheless, in regions south of 60° N, Δ_A is sometimes close to $(\delta_a - \delta_r)$ and in such conditions a plot of δ_a versus $1/C_a$ yields δ_r at $1/C_a = 0$ (ref. 39). For air over Switzerland, a mean value of −16.4‰ (PDB-CO_2) was calculated[32]. Our model gives an average δ_r of −14.7‰ and an average Δ_A of 19.2‰ for that region.

The most important conclusion of this work is that, not only do terrestrial fluxes have a different effect on δ_a from oceanic fluxes, but different biomes also have markedly different discriminations (Fig. 3). Accurate measurements of rates of change in δ_a in a comprehensive global network together with appropriate meteorological data should therefore help to resolve the present conflicts about the relative role of the oceans and the terrestrial biosphere in the net uptake of CO_2 (equation (3)). They should also allow the identification of components of the terrestrial biota currently acting as net carbon sinks. □

Received 10 November 1992; accepted 22 March 1993.

1. Francey, R. J. & Tans, P. P. *Nature* **327,** 495–497 (1987).
2. Craig, H. & Gordon, L. I. in *Proc. Conf. Stable Isotopes in Oceanographic Studies and Paleotemperatures* 9–130 (Laboratory of Geology and Nuclear Science, Pisa, 1965).
3. Farquhar, G. D., Hubick, K. T., Condon, A. G. & Richards, R. A. in *Stable Isotopes in Ecological Research* (eds Rundel, P. W., Ehleringer, J. R. & Nagy, K. A.) 21–40 (Springer, New York, 1989).
4. Bottinga, Y. & Craig, H. *Earth planet. Sci. Lett.* **55,** 285–295 (1969).
5. Merlivat, L. *J. chem. Phys.* **69,** 2864–2871 (1978).
6. Cowan, I. R. *Adv. Bot. Res.* **4,** 117–228 (1977).
7. O'Neil, J. R., Adami, L. H. & Epstein, S. *J. Res. U.S. geol. Survey* **3,** 623–624 (1975).
8. Farquhar, G. D., Ehleringer, J. R. & Hubick, K. T. *A. Rev. Plant Physiol. Plant molec. Biol.* **40,** 503–537 (1989).
9. Lloyd, J., Syvertsen, J. P., Kriedemann, P. & Farquhar, G. D. *Plant Cell Environ.* **15,** 873–900 (1992).
10. Yakir, D., Berry, J. A., Giles, L. J., Osmond, C. B. & Thomas, R. B. in *Physiological Processes from the Leaf to the Globe* (eds Ehleringer, J. R. & Field, C. B.) 323–338 (Academic, San Diego, 1993).
11. Yurtsever, Y. & Gat, J. R. in *Stable Isotope Hydrology: Deuterium and Oxygen-18 in the Water Cycle* (eds Gat, J. R. & Gonfiantini, R.) 103–142 (IAEA, Vienna, 1981).
12. Hesterberg, R. & Siegenthaler, U. *Tellus* **B43,** 197–205 (1991).
13. International Atomic Energy Agency, *Environmental Isotope Data No. 1: World Survey of Isotope Concentration in Precipitation* Vols 7–9 (1983–1988).
14. Oort, A. *Natn. Oceanic Atmos. Admin. Prof. Pap.* **14** (1983)
15. Shea, D. J. *Tech. Note natn. Cent. atmos. Res. TN-269 + STR* (NCAR, Boulder, 1986).
16. Cogley, J. G. *Tech. Note 85-4* (Trent Univ., Peterborough, Ontario, 1985).
17. Jouzel, J. *et al. J. geophys. Res.* **96,** 7495–7507 (1991).
18. Lloyd, J. *Austr. J. Plant Physiol.* **18,** 649–660 (1991).
19. Cowan, I. R. & Farquhar, G. D. *Symp. Soc. exp. Biol.* **31,** 471–505 (1977).
20. Henderson-Sellers, A., Wilson, M. F., Thomas, G. & Dickinson, R. E. *Natn. Cent. for atmos. Res. Tech. Note-272 + STR* (1986).
21. Lieth, H. in *Primary Productivity of the Biosphere* (eds Lieth, H. & Whittaker, R. H.) 237–263 (Springer, Berlin, 1975).
22. Taylor, J. A., Brasseur, G. P., Zimmerman, P. R. & Cicerone, R. J. *J. geophys. Res.* **96,** 3013–3044 (1991).

23. Poorter, H., Remkes, C. & Lambers, H. *Pl. Physiol.* **94,** 621–627 (1990).
24. Masle, J., Farquhar, G. D. & Gifford, R. M. *Austr. J. Plant Physiol.* **17,** 465–487 (1990).
25. Jarvis, P. & Leverenz, J. W. in *Encyclopaedia of Plant Physiology* Vol. 12D (eds Lange, O. L., Nobel, P. S., Osmond, C. B. & Zeilger, H.) 233–280 (Springer, Berlin, 1983).
26. Medina, E. & Klinge, H. in *Encyclopaedia of Plant Physiology* Vol. 12D (eds Lange, O. L., Nobel, P. S., Osmond, C. B. & Ziegler, H.) 281–304 (Springer, Berlin, 1983).
27. Poorter, H. in *Causes and Consequences of variations in Growth Rate and Productivity of Higher Plants* (eds Lambers, H., Cambridge, M. L., Konings, H. & Pons, T. L.) 49–68 (SPB Academic, The Hague, 1989).
28. Zundel, G., Miekeley, W., Grisi, B. M. & Försel, H. *Radiat. Envir. Biophys.* **15,** 203–212 (1978).
29. Barnes, C. J. & Allison, G. B. *J. Hydrol.* **100,** 143–176 (1988).
30. Bariac, T., Rambal, S., Jusserand, C. & Berger, A. *Agric. For. Meteor.* **48,** 263–283 (1989).
31. Bariac, T., Jusserand, C. & Mariotti, A. *Geochim. cosmochim. Acta* **54,** 413–424 (1990).
32. Friedli, H., Siegenthaler, U., Rauber, D. & Oeschger, H. *Tellus* **B39,** 80–88 (1987).
33. Tans, P. P. *Tellus* **B32,** 464–469 (1980).
34. Houghton, J. T., Jenkins, G. J. & Ephraums, J. J. *Climate Change: The IPCC Scientific Assessment* (Cambridge University Press, UK, 1990).
35. Levitus, S. *Climatological Atlas of the World Ocean.* (Natn. Oceanic Atmosp. Admin. Prof. Pap. **13,** 1981).
36. Friedman, I. & O'Neil, J. R. in *US geol. Surv. Prof. Paper.* 440-KK (1977).
37. O'Neil, J. R. & Adami, L. H. *J. phys. Chem.* **73,** 1553–1558 (1969).
38. Allison, G. B., Colin-Kaczala, C., Filly, A. & Fontes, J. C. H. *J. Hydrol.* **95,** 131–141 (1987).
39. Keeling, C. D. *Geochim. cosmochim. Acta* **24,** 277–298 (1961).
40. Mook, W. G., Koopmans, M., Carter, A. F. & Keeling, C. D. *J. geophys. Res.* **88,** 10915–10933 (1983).

ACKNOWLEDGEMENTS. We thank I. R. Cowan, C. B. Osmond, J. A. Berry, J. R. Evans, J. E. Robertson and S. von Caemmerer for comments, R. Francey, A. Chivas and J. Olley for isotope standards, R. Koster for simulations of $\delta^{18}O$ of water vapour in relation to precipitation and I. Watterson for humidity fields.

A new species of living bovid from Vietnam

Vu Van Dung, Pham Mong Giao, Nguyen Ngoc Chinh, Do Tuoc, Peter Arctander & John MacKinnon*†

Forest Inventory and Planning Institute, Ministry of Forestry, Hanoi, Vietnam
* Asian Bureau for Conservation, 18/E Capital Building, 175–191 Lockhart Road, Wanchai, Hong Kong

IN May 1992 a joint survey by the Ministry of Forestry and World Wide Fund for Nature of the Vu Quang Nature Reserve, Ha tinh province, found three sets of long straight horns of a new bovid (Mammalia, Artiodactyla) in hunters' houses[1]. None of the specimens had dentition. On four follow-up visits by Vietnamese scientists new specimens were discovered and surveys of forests in neighbouring Nghe an province revealed more localities and some partial specimens. In all, we have examined more than 20 specimens. Three have complete upper skulls and dentitions, two have lower jaws and dentitions. Three complete skins have been collected. The specimens are distinct in appearance, morphology and DNA sequence and cannot be ascribed to any known genus. Only two bovid genera are known from this part of Asia, *Bos* and *Naemorhedus* = *Capricornis*[2,3]. A new genus and species are therefore described. Such a discovery is of great significance. It has been more than 50 years since any comparable find of a large mammal species has been made; the last being the kouprey *Bos* = *Novibos sauveli*, another Indochinese bovid (Urbain, 1937). Moreover, the bovids (cattle, goats and antelopes) are a mammal family of great value to mankind. Many species have proven or potential value for domestication or cross-breeding. A three-month field study is planned to observe the living animal.

FORMAL DESCRIPTION

Family Bovidae
Subfamily Bovinae
Tribe ? Boselaphini
Genus *Pseudoryx*, gen. nov.

Diagnosis. *Pseudoryx* differs significantly from all described genera in appearance, morphology, cranial and dental features and DNA. The long, smooth, almost straight, slender horns, elongated premolars, large face gland and distinctive colour pattern are diagnostic.

Description. See under species description.

Etymology. The name reflects the superficial similarity to *Oryx* in having long straight horns slightly recurved in profile, with bold black and white facial markings, while clarifying that the animal is not closely related to *Oryx*.

Type species. *P. nghetinhensis*, sp. nov.

Pseudoryx nghetinhensis sp. nov.

Diagnosis. The only species of the genus. Diagnosis as for genus.

Description. The total body weight of the adult is estimated at about 100 kg. Total length from nose to anus is about 1.5 m. Height at the shoulder is about 80–90 cm. Length from spine to front foot across preserved skin is 96 cm. Tail is short, about 13 cm of bone with fluffy black tassle. Ear length is quite short at about 10 cm. Skull length varies between 32 and 36.5 cm.

The skull is highly bridged in the nasal area. The horns are long, almost straight, smooth, almost parallel in females, and only moderately diverging in males. They are almost circular in cross-section, with horn cores extending close to the tip. Horn length varies from 32 to 52 cm, with a mean (18) = 41 cm. Width between tips varies from 7.5 to 20 cm, with mean (17) = 13.3 cm. Both length and distance between the tips show a bimodal distribution, with inferred males having longer more divergent horns than females. The insertion of the horns is much wider than for goat-antelopes (such as the serow *Naemorhedus sumatraensis*; Fig. 3*b*), similar to the mountain anoa *Bubalus quarlesi*, but narrow for cattle. Internal width between horns basally varies from 3.0 to 4.0, with a mean (6) = 3.7 cm. The outer width across the horns basally varies from 10 to 12, with a mean (6) = 10.5 cm. The basal 7 cm shows narrow annuli, but

FIG. 1 Photographs of Vu Quang bovid: *a*, type specimen FIPI/MVQ001; *b*, stuffed skin of another individual.

† To whom correspondence should be addressed.